

ENERGETICS APPROACH TO FATIGUE BEHAVIOR OF WOODEN JOINT USING DOUBLE-SIDED ADHESIVE TAPE

Keita Ogawa

Graduate Student
E-mail: ogawa.keita@e.mbox.nagoya-u.ac.jp

Ryohei Suzuki

Graduate Student
Department of Biosphere Resources Science
Graduate School of Bioagricultural Sciences
Nagoya University
Furo-cho, Chikusa-ku, Nagoya, Aichi 464-8601, Japan
E-mail: suzuki.ryohei@h.mbox.nagoya-u.ac.jp

Satoshi Fukuta

Senior Researcher
Industrial Research Center
Aichi Center for Industry and Science Technology
1-157-1 Onda-cho, Kariya, Aichi 448-0013, Japan
E-mail: fukuta@aichi-inst.jp

Mariko Yamasaki

Associate Professor
E-mail: marikoy@agr.nagoya-u.ac.jp

*Yasutoshi Sasaki**

Professor
Department of Biosphere Resources Science
Graduate School of Bioagricultural Sciences
Nagoya University
Furo-cho, Chikusa-ku, Nagoya, Aichi 464-8601, Japan
E-mail: ysasaki@nagoya-u.jp

(Received February 2016)

Abstract. The authors previously studied the possibility of the use of industrial double-sided adhesive tape as a method for jointing wooden panel to wooden framework. The mechanical performance of joints formed by such methods is comparable with that of nailed joint under static load conditions. However, the mechanical performance of such joints has not been evaluated under cyclic load conditions. This study was conducted to investigate this aspect of their performance. Double-shear specimens were prepared by bonding wooden panel to wooden framework using two types of adhesive tape with different substrates. Specimens were also prepared with wooden dowels to strengthen their jointing performance. The joint specimens were subjected to cyclic shear loading testing. The results of the tests were analyzed from an energetics perspective, and the shear deformability of the specimens at failure was estimated. The test results indicated that both the specimens formed using adhesive tape and those formed using wooden dowels had fatigue properties comparable with nailed joint specimens. A tendency for the shear deformability caused by cyclic loading to increase with the stress level was observed. It was possible to estimate the shear deformability by evaluating the energy absorption capacity of the joints from an energetics standpoint.

Keywords: Wooden joint, adhesive tape, cyclic shear loading, fatigue, strain energy, deformability.

* Corresponding author

INTRODUCTION

Wooden buildings are found throughout the world, supporting the daily lives of people as dwellings. To ensure the safety of the people who use these buildings, building mechanical performance must be understood. In Japan in particular, earthquakes, typhoons, and other disasters occur almost every year, severely damaging wooden buildings. Repeated disasters of these types expose wooden buildings to cyclic loading by external forces. It is therefore important to examine the remaining performance of load-bearing elements of wooden buildings during and after repeated loading. A number of studies on the fatigue properties of wooden joints have been carried out. For example, Wakashima and Hirai (1993) applied cyclic shear loading to a nailed joint to measure the change in its energy absorption ability with repeated loading. The energy absorption ability was found to converge under conditions of constant load control or constant displacement control. Chui et al (1998) used the finite element method to reproduce the load-slip displacement curve of a nailed joint subjected to cyclic loading. Li et al (2012) performed shear fatigue testing of wooden joints using nails and reported that the shear behavior of the joint changed between when testing began and when fatigue failure occurred. At the beginning of fatigue testing and immediately before failure, the increase in the number of cycles was accompanied by an increase in the dissipated energy per cycle. The researchers proposed an energetics-based formula for prediction of the fatigue life of the joint.

The authors have previously studied the possibility of using industrial double-sided adhesive tape to bond wooden panels to wooden framework or to strengthen such joints using wooden dowels. These types of joints could conceivably be used as substitutes for nailed joints in panel-sheathed shear walls. Wooden structural elements formed using this joint method can be counted on to be greatly airtight and to provide greater levels of soundproofing and insulation performance than those formed using the nailed joint method. Fukuta et al (2013) performed

double-shear testing to investigate the mechanical performance of joints formed using this method and found that joints formed using double-sided adhesive tape had greater shear capacities than nailed joints, which suggests that the former can be effective joints. In addition, when a panel-sheathed shear wall was constructed using this joint method and subjected to in-plane shear testing, the results clearly showed that its performance was equal to that of a wall constructed using nailed joints and that it is possible to estimate its strength theoretically (Ogawa et al 2015).

Studies such as those mentioned have verified that the mechanical performance of this type of joint is adequate for use with the bearing elements of a wooden building under static loading conditions. However, the mechanical performance of this type of joint under dynamic load conditions has not been verified. In this study, cyclic shear loading was applied to joint specimens formed using double-sided adhesive tape and to specimens formed using wooden dowels to verify the fatigue behavior of these types of joints experimentally. An effort was also made to apply the energetics approach to estimating deformability of these types of joints at failure.

MATERIALS AND METHODS

Joint Specimens

Double-shear specimens of joints were prepared in compliance with the Japan Agricultural Standards (2013). Figure 1a shows a specimen. The base material used was air-dried Japanese cedar (*Cryptomeria japonica* D.DON) with dimensions of $38 \times 89 \times 300$ mm (moisture content $13.9\% \pm 1.9\%$, density 395.1 ± 13.4 kg/m³, average value \pm standard deviation). The side panels used were four-ply Japanese cedar structural plywood (Japan Agricultural Standards structural plywood, type special, class 2; moisture content $13.4\% \pm 1.4\%$; density 476.3 ± 14.6 kg/m³) with dimensions of $12 \times 100 \times 300$ mm. The connectors for the base material and side panels were two types of acrylic-resin double-sided adhesive tape, R230 and DF5680A (Toyo Ink Co., Ltd., Tokyo, Japan).

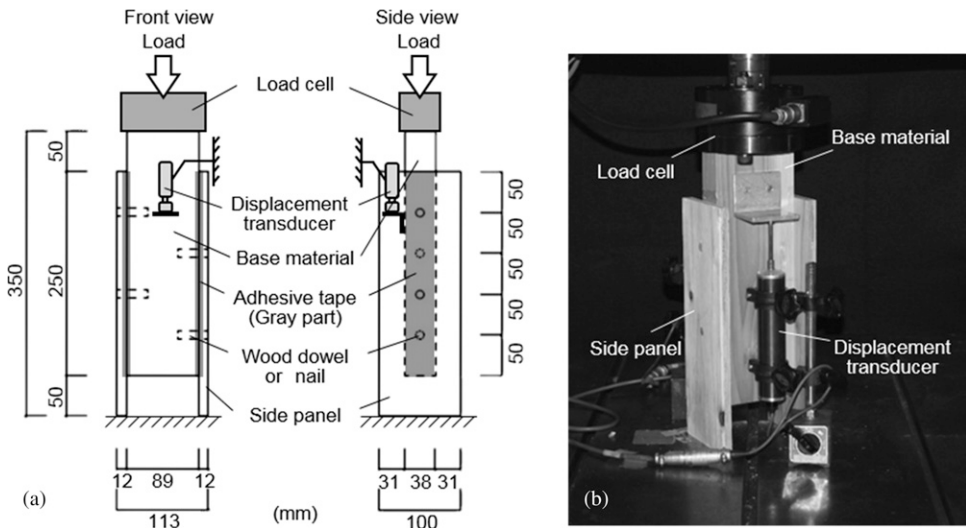


Figure 1. Specimen and loading method.

R230 has a nonwoven fabric as its substrate and is 145 μm thick. The specimens made using this tape were denoted type T1. DF5680A has a polyolefin foam as its substrate and is 1140 μm thick. The specimens made using this tape were denoted type T2. Specimens with each of these two types of tape were also prepared using dowels (10 mm in diameter and 36 mm in length) made of beech wood (*Fagus crenata* Blume) for the improvement of initial stiffness. These specimens were denoted T1D and T2D, respectively. A compressive pressure of 1.0 MPa was applied to the adhesive tape for 10 s. The specimens were then left to cure in the laboratory for at least a week. When a dowel was also used, after the adhesive tape was applied, a drill was used to bore a dowel hole with a diameter of 9.5 mm and the wooden dowel was hammered

into the hole. For comparison, specimens formed with a nailed joint (CN50) were also prepared (type N). Table 1 summarizes the properties of the five types of specimens.

Static Testing and Cyclic Load Testing

First, static testing was performed to determine the static strength of the five types of specimens. An electrohydraulic servo fatigue testing machine (EHF-UB5-10L, Shimadzu Co., Kyoto, Japan) was used to carry out the static loading testing, as shown in Fig 1b. Each specimen was placed on top of a rigid surface, and compression loading of the top of the base material was performed allowing shear force to act on the joint surface. The shear stress was determined by dividing the load magnitude by the joint surface area.

Table 1. Connecting material used to make the specimens.

Specimen type	Connector		
	Adhesive tape ^a	Wood dowel	Nail
T1	R230 (145 μm thick)	—	—
T2	DF5680A (1040 μm thick)	—	—
T1D	R230 (145 μm thick)	Beech wood (φ10 mm, 36 mm long)	—
T2D	DF5680A (1040 μm thick)	Beech wood (φ10 mm, 36 mm long)	—
N	—	—	CN50

^a Manufactured by Toyo Ink Co. Ltd., Tokyo, Japan.

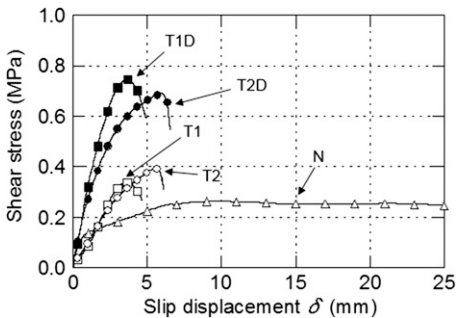


Figure 2. Shear stress-slip displacement curve obtained from static testing.

The slip displacement between the base material and the side panels was measured with a strain-gauge-type displacement transducer (CDP-50, Tokyo Sokki Kenkyujo, Co., Ltd., Tokyo, Japan). The loading rate was 2.4 mm/min. After the maximum stress τ_{\max} was reached, loading was continued until the stress reached 80% of τ_{\max} . Five specimens of each type were subjected to static testing.

Cyclic load testing (Fig 1b) was performed in the same manner as previously described, except that cyclic loading was performed under load control using a pulsating triangular wave load form and a load frequency of 0.5 Hz. Four stress levels (SLs), 60%, 70%, 80%, and 90% of the maximum stress τ_{\max} measured in static testing, were set. Three specimens were tested under each set of conditions. The time of separation of the side panels from the base material was considered to be failure, and cyclic loading was continued until failure occurred. The tests were performed in an environment with a room temperature of 25°C and humidity of 55%. The load and slip displacement sampling frequency during the testing was 20 Hz.

RESULTS AND DISCUSSION

Static Strength

Figure 2 shows an example of a stress-slip displacement curve obtained by static testing. Table 2 shows the strength property values obtained from the stress-slip displacement curve. The maximum stress τ_{\max} is the strength, which is the SL standard in the cyclic load testing. The specimens made with double-sided adhesive tape (types T1 and T2) exhibited maximum stress values greater than those of the nailed joint specimens (type N). The specimens formed using double-sided tape all reached maximum stress τ_{\max} when the slip displacement was between 3 and 5 mm, but the nailed specimens maintained their bearing capacity until the slip displacement exceeded 20 mm. A comparison of the two types of adhesive tape (T1 and T2) showed that the slip at failure (when the stress fell to 80% of τ_{\max}) was greater for T2, which had the thicker substrate.

Turning to the reinforcing effects of the wooden dowel shown in Fig 2 (T1 vs T1D and T2 vs T2D), the specimens containing wooden dowels (Types T1D and T2D) were found to withstand higher stress from the first stage of loading onward. The stress greatly exceeded the stress levels withstood by specimens of types T1 and T2, clearly demonstrating the reinforcing effects of using wooden dowels in conjunction with adhesive tape. However, maximum stress was reached when the slip displacement was between 3 and 5 mm, and the use of wooden dowels did not have an evident effect on deformability.

Fatigue Strength

Figure 3 shows an example of a stress-slip displacement curve obtained from the cyclic load

Table 2. Static testing results.

Specimen type	Maximum stress τ_{\max} (MPa)	Strain energy V_{sta} (MPa-mm)	Rigidity K (MPa/mm)
T1	0.339 ± 0.068	0.697 ± 0.135	1.72 ± 0.38
T2	0.390 ± 0.008	1.347 ± 0.029	1.88 ± 0.03
T1D	0.753 ± 0.038	1.800 ± 0.180	6.31 ± 0.50
T2D	0.688 ± 0.004	2.711 ± 0.199	5.74 ± 1.45
N	0.262 ± 0.004	2.893 ± 1.468	2.89 ± 0.39

The values in the table are averages \pm standard deviations.

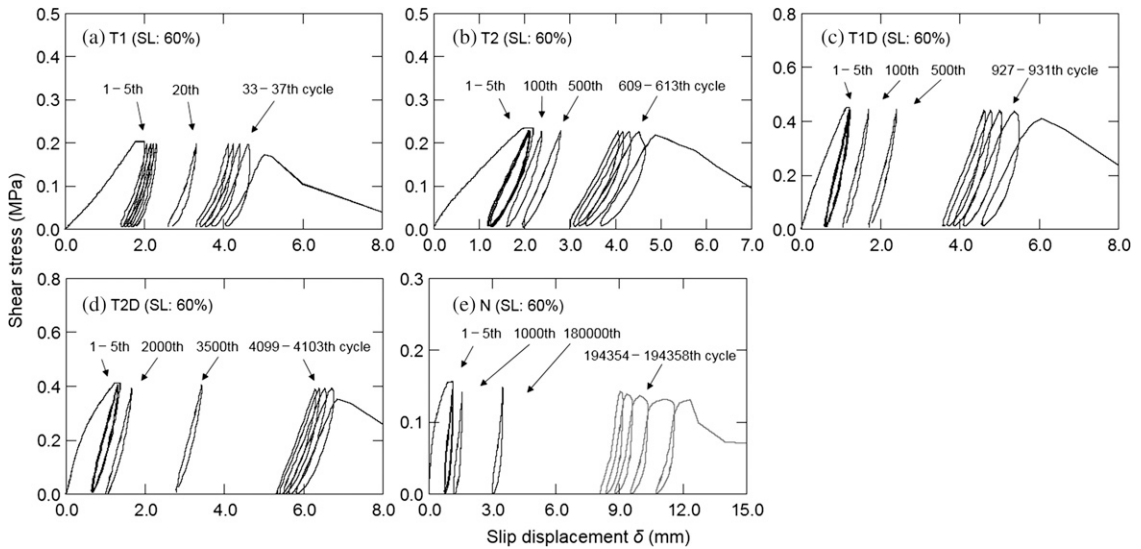


Figure 3. Shear stress-slip displacement curve obtained from cyclic load testing: (a) T1 (b) T2 (c) T1D (d) T2D (e) N.

testing. For example, Fig 3b shows a curve obtained from cyclic testing of a type T2 specimen at a SL of 60%, and the fatigue life N_f was 613 cycles. Figure 3 illustrates the results for the 1st to 5th, 100th, 500th, and 609th to 613th cycles. The first cycle increased the shear stress and the slip displacement, but at this stress level, only elastic behavior was exhibited and yield did not occur. When unloading started, slip displacement recovery began and a hysteresis loop was plotted at that time. When unloading was completed, the displacement did not completely recover, revealing slight residual displacement. As the number of cycles increased, the loop shifted to the right, indicating an accumulation of residual displacement.

When the number of load cycles reached the fatigue life N_f , the base material and side panels of the specimens separated. The failure modes at this time are shown in Fig 4 by type. In the cases of types T1 and T2, the adhesive tape peeled off without wood failure being observed in any of the specimens. In the cases of types T1D and T2D, which contained wooden dowels, adhesive tape separation and breakage of the wooden dowel occurred simultaneously (Fig 4f). In the case of type N, shear failure of the nail was observed (Fig 4g).

Figure 5a shows the relationships between SL and fatigue life N_f (the S-N relationships) for all of the specimens. In the cases of types T2 (\circ), T1D (\blacksquare), T2D (\bullet), and N (\triangle), significant regressions were obtained on a semilogarithmic scale. For type T1 (\square), conversely, the regression was not significant. When results for specimens formed using only adhesive tape were compared with results for specimens formed using both adhesive tape and wooden dowels (ie T1 vs T1D and T2 vs T2D), the results and regression lines for the specimens with wooden dowels plotted on the long-life side of the figure indicated that the use of a wooden dowel can be counted on to increase the fatigue life. The plot for type N specimens was located further along the long-life side than the results for the other types of specimens.

As Fig 5a shows, the ordinate intercepts for almost all of the regression lines exceeded 100%. This is assumed to be a result of the difference between the static and cyclic loading rates (2.4 mm/min and 33.6-140.4 mm/min, respectively) (McNatt 1978). For the type N specimens, when a cyclic loading test at an SL greater than 100% was performed, the regression line had a bilinear shape, with a boundary between 90% and 100%, as shown in Fig 5a. This suggests that the behavior

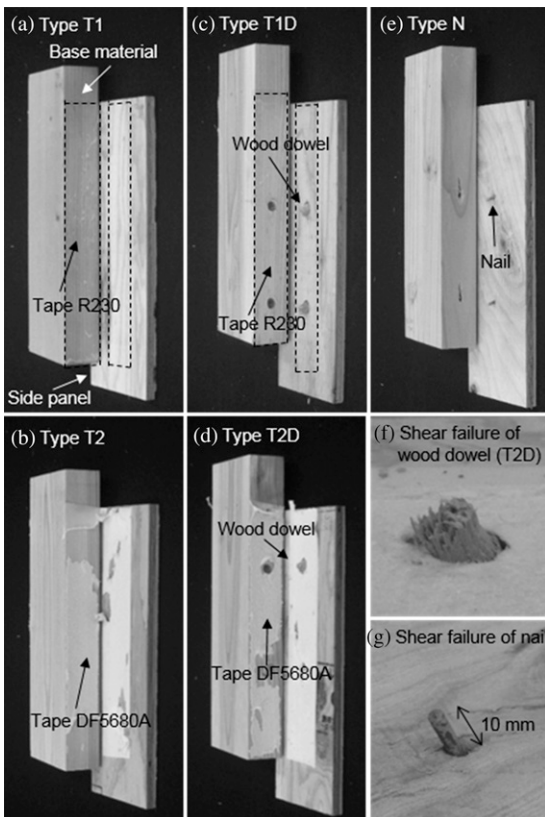


Figure 4. Failure modes in cyclic load testing: (a) T1 (b) T2 (c) T1D (d) T2D (e) N (f) wooden dowel (g) nail. Tape R230 was still applied in the range enclosed by the dotted line even after failure ([a] and [c]).

of a nailed joint under cyclic loading changes with the boundary between SL 90% and 100%.

As stated in the Introduction, the joint method that combines double-sided adhesive tape with a

wooden dowel is expected to be applicable to panel-sheathed shear walls, and evaluation of the mechanical performance of this type of joint under cyclic loading is important. Figure 5b shows the relationship of the applied stress τ_a to the fatigue life N_f (the number of cycles to failure). The plots for types T1D, T2D, and N are almost all on the same straight line. Hence, if the same applied stress to N specimen ($\tau_a = 0.2-0.3$) is given to T1D and T2D specimens, it is expected that the T1D and T2D specimens are plotted near N specimens' plots. The result shows that the S-N relationship (in terms of performance under cyclic shear loading) of joints with adhesive tape and wooden dowels was similar to that of nailed joints. Nailed joints are typically used in panel-sheathed shear walls. Therefore, joints with adhesive tape and wooden dowels can also be considered to be applicable to shear walls.

Strain Energy

Based on the stress–slip displacement curve (Fig 3) obtained by cyclic load testing, an energetics-based analysis was attempted. The area shown in dark grey in Fig 6 was defined as the strain energy per cycle V_c , and this was calculated for each number of cycles. Figure 7a shows an example of the change in strain energy with increasing number of cycles. As Fig 7a shows, a high strain energy V_c appeared at the first cycle, but at the second cycle and thereafter, the strain energy V_c decreased. And, just before fatigue failure, the strain energy became an almost constant value.

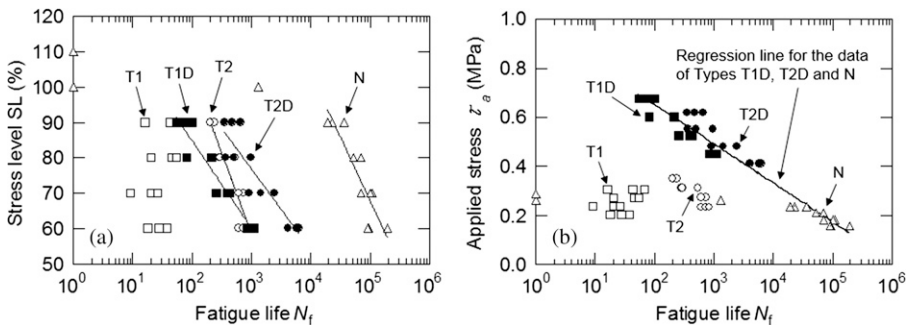


Figure 5. S-N lines: (a) stress level–fatigue life relationship (b) applied stress–fatigue life relationship.

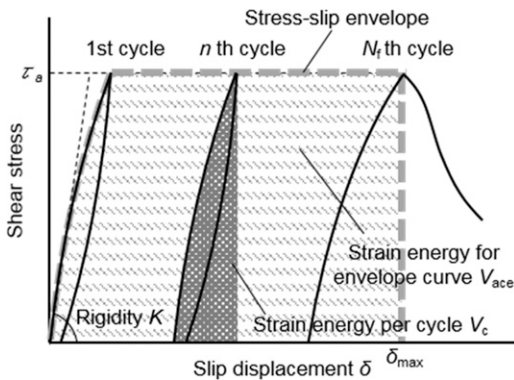


Figure 6. Strain energy calculation method and stress–slip displacement envelope definition.

This indicates that the energy absorption ability under an external force was high during the initial loading. As the end of the fatigue life neared, the strain energy V_c tended to increase. Mechanisms such as the following are considered to be responsible for this tendency. First, it is thought that whenever cyclic loading is applied to these types of joints, local separation of the tape adhesive surface and slight nail damage occur, and as the number of loading cycles increases, these effects accumulate. When the mechanical burden on the remaining portion of the specimen to which the adhesive tape still adheres effectively exceeds a certain level, the stress–slip displacement relationship during loading reveals the occurrence of plastic behavior, and as it nears its fatigue life, the strain energy V_c increases. This tendency for the strain energy V_c to increase as the end of the fatigue life is neared has been

noted in various fatigue tests of wood and wood-based materials (Sugimoto et al 2007). In addition, comparisons of type T1 with type T1D and type T2 with type T2D showed that the use of a wooden dowel increased the strain energy V_c because the applied stress was high.

The relationship between the cumulative strain energy V_{acf} from the start of loading to fatigue failure and the fatigue life N_f is illustrated in Fig 7b. For all joint types considered in this study, a significant positive slope to the regression line was obtained on a log-log plot. Similar results have been reported for various fatigue tests of wood and wood-based materials (Sasaki et al 2014; Watanabe et al 2014). As Fig 7b shows, under conditions that increase the fatigue life N_f (low stress levels, for example), the cumulative strain energy V_{acf} required to cause fatigue failure is greater than it is under conditions that decrease N_f .

The thick dashed line in Fig 6 represents the envelope from the first load to the end of the fatigue life for the stress–slip displacement curve obtained for cyclic loading (Gong and Smith 2005; Sasaki et al 2014). The strain energy of this envelope, V_{ace} , is defined by the following equation:

$$V_{ace} = \int_0^{\delta_{max}} (\text{stress} - \text{slip envelope}) d\delta \quad (1)$$

For the stress–slip displacement curve obtained for static loading, shown in Fig 2, the strain energy from the start of loading to the maximum stress is obtained. This is shown in Table 2 as the static strain energy V_{sta} .

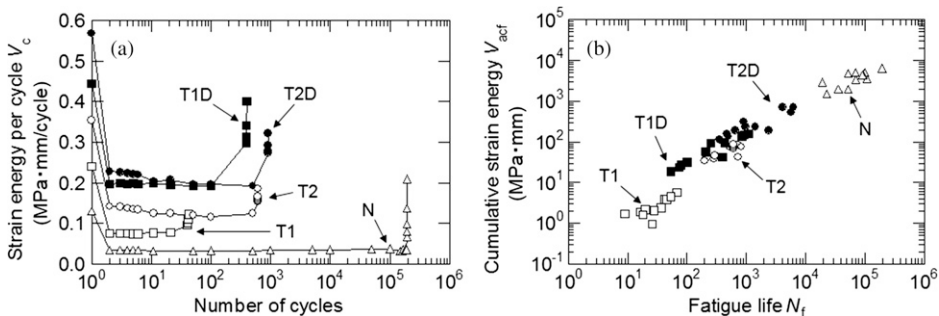


Figure 7. Strain energy analysis results: (a) relationship of strain energy per cycle to number of cycles (b) relationship of cumulative strain energy to fatigue life.

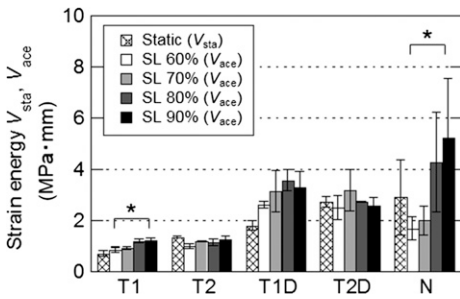


Figure 8. Strain energy from static testing and envelope strain energy at each stress level. The height of the bar indicates the average value, and the error bar indicates the standard deviation. * Significant difference at 0.05.

Figure 8 shows the relationship of the static strain energy V_{sta} to the envelope strain energy V_{ace} for each stress level. According to past research on bending fatigue testing of wood (Sasaki et al 2014), the envelope strain energy V_{ace} can be considered to be almost constant regardless of the SL, and its value can be estimated as approximately 1.5 times the static strain energy V_{sta} ($V_{ace}/V_{sta} = 1.5$). As Fig 8 shows, the cumulative strain energy V_{ace} values of the type T1 and N joints differed depending on the SL. An analysis of variance of V_{ace} was performed for each joint type, and it was confirmed that the V_{ace} values of types T1 and N differed depending on SL (at a significance level of 0.05). No differences for different SL levels occurred for types T2, T1D, or T2D, which is consistent with results reported in an earlier study (Sasaki et al 2014). In addition, when V_{sta} and V_{ace} were compared, it was found that the trends according to specimen type were diverse and that the $V_{ace}/V_{sta} = 1.5$ approximation suggested in an earlier study (Sasaki et al 2014) did not hold. In the cases of types T1 and T1D for example, the value of V_{sta} was lower than any value of V_{ace} , but the value was almost identical for types T2 and T2D. It assumed that this reflects differences among the substrates of the tapes.

Slip Displacement at Fatigue Failure

Evaluation of the slip displacement δ_{max} at fatigue failure is presumed to be important to the application of these joint methods to the structural elements of a building (Ogawa et al

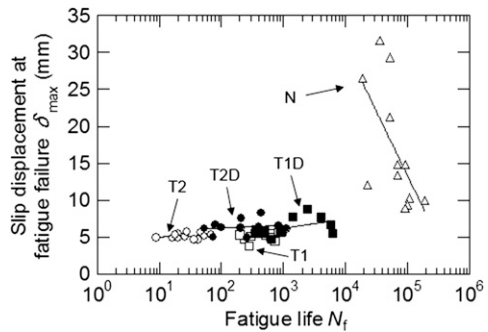


Figure 9. Relationship of slip displacement at fatigue failure to fatigue life.

2015). Figure 9 shows the relationship of fatigue life N_f to slip displacement δ_{max} at fatigue failure. Figure 9 shows that δ_{max} for the nailed joint specimens (type N) was approximately 10-30 mm and that the relationship fell to the right with respect to fatigue life. This is a result of the fact that, at high stress levels, when the fatigue life was reached while nails maintained support from the base material, the embedding displacement into the base material was high, but at low stress levels, the nail reached fatigue failure while embedding displacement remained low. Therefore, it was assumed that the fatigue life increased as δ_{max} remained low. The values of δ_{max} for the specimens using adhesive tape (types T1, T2, T1D, and T2D) were approximately 4.0-8.0 mm, which was much lower than in the case of a nailed joint. The value was almost constant compared with that of type N, but a detailed examination showed that δ_{max} increased slightly as the fatigue life increased and that the deformability was greater under long-fatigue-life conditions.

With respect to the slip displacement δ_{max} at fatigue failure, as Fig 6 shows, the shape of the stress–slip envelope is almost a trapezoid. Therefore, the relationship to the envelope strain energy V_{ace} can be approximated as shown by the following equation:

$$V_{ace} \approx \frac{1}{2} \tau_a \left(2\delta_{max} - \frac{\tau_a}{K} \right) \tag{2}$$

In this equation, τ_a is the applied stress during the fatigue test. If the ratio α of V_{ace} to V_{sta}

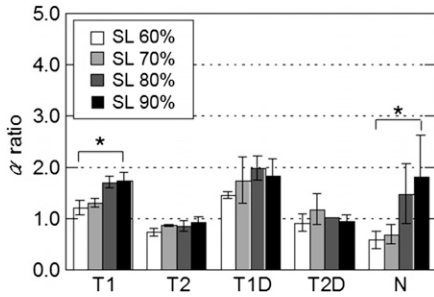


Figure 10. Value of α at each stress level. The height of the bar indicates the average value, and the error bar indicates the standard deviation. * Significant difference at 0.05.

($=V_{ace}/V_{sta}$) is defined, the previous equation can be rewritten as

$$\delta_{max} = \frac{\alpha \cdot V_{sta}}{\tau_a} + \frac{\tau_a}{K} \quad (3)$$

According to this equation, knowing the value of α permits estimation of the slip displacement δ_{max} at fatigue failure based on the rigidity K and the strain energy V_{sta} determined from static testing. In this study, we attempted to estimate the slip displacement at fatigue failure using the previous equation, and we denoted this estimate by δ_{me} .

The rigidity K was calculated based on the proportional range of the stress–slip displacement curve from static testing shown in Fig 2 and is shown in Table 2. The ratio α of V_{ace} to V_{sta} ($=V_{ace}/V_{sta}$) was calculated for each stress level and each joint type. The values are shown in Fig 10. An analysis of variance showed that SL had a significant influence (at the 0.05 significance level) on the value of the ratio α for types T1 and N but not for types T2, T1D, or T2D.

The values shown in Table 2 and Fig 10 (V_{sta} , K , α) were used to estimate δ_{me} , and the ratio of this to the experimental δ_{max} was calculated. Figure 11 and Table 3 show the results for each stress level and each joint type. Figure 11 shows that the ratio of the estimated value to the experimental value was approximately 1.0 and that it is possible to estimate the slip displacement at fatigue failure accurately, based on the results of static testing. Evaluation of the amount of slip

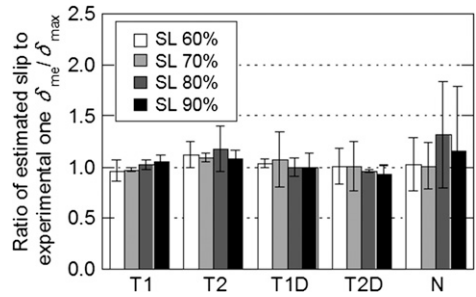


Figure 11. Ratio of estimated value to experimental value for slip displacement at fatigue failure. The height of the bar indicates the average value, and the error bar indicates the standard deviation.

displacement caused by cyclic loading is an important aspect of the evaluation of the feasibility of applying adhesive tape to buildings. When the ductility of structural elements in particular is considered, it is important to evaluate the limits of deformation. As Fig 10 shows, in the cases of types T2, T1D, and T2D, the value of α can be considered almost constant, regardless

Table 3. Experimental and estimated slip displacement at fatigue failure.

Specimen type	SL ^a (%)	δ_{max}^b (mm)	δ_{me}^c (mm)	δ_{me}/δ_{max}
T1	90	4.95 (0.33)	5.20	1.05
	80	5.39 (0.25)	5.48	1.02
	70	4.95 (0.11)	4.80	0.97
	60	5.20 (0.53)	4.97	0.96
T2	90	5.11 (0.33)	5.52	1.08
	80	4.66 (0.79)	5.36	1.15
	70	5.29 (0.20)	5.77	1.09
	60	4.98 (0.58)	5.53	1.11
T1D	90	5.84 (0.72)	5.79	0.99
	80	6.81 (0.66)	6.73	0.99
	70	6.53 (1.66)	6.68	1.02
	60	6.22 (0.26)	6.40	1.03
T2D	90	5.26 (0.44)	4.88	0.93
	80	5.88 (0.10)	5.64	0.96
	70	7.38 (1.60)	7.17	0.97
	60	6.63 (1.10)	6.53	0.99
N	90	23.34 (10.14)	22.59	0.97
	80	21.33 (7.97)	25.31	1.19
	70	11.49 (2.96)	11.15	0.97
	60	11.25 (3.19)	10.99	0.98

^a SL, stress level.

^b Experimental slip displacement at failure. Parentheses mean standard deviation.

^c Estimated slip displacement at failure.

of the stress level SL (type T2 $\alpha = 0.8$, type T1D $\alpha = 1.8$, and type T2D $\alpha = 1.0$). In the cases of types T1 and N, the value of α was influenced by SL, and it can be surmised that the value of α varies within the range of SL = 70-80%. Thus, it is considered to be desirable that when estimating δ_{\max} , the value of α should be varied depending on SL.

CONCLUSIONS

To assess the fatigue behavior of joints formed using industrial double-sided adhesive tape under cyclic loading, cyclic load testing was performed using double-shear specimens and an energetics-based analysis was conducted. Based on the relationship of SL to fatigue life, it was concluded that joints formed using both adhesive tape and wooden dowels exhibited S-N relationships similar to those of nailed joints. The result of an energy analysis showed that the strain energy was high for the first cycle, then decreased starting with the second cycle, and ultimately became almost constant near the fatigue life of the joint. This suggests that the energy absorbance ability under the application of external forces was high for the first load. The energy calculated from the envelope curve of the stress-slip displacement relationship was not influenced by SL for three of the joint types T2, T1D, and T2D. The slip displacement at fatigue failure decreased as the fatigue life increased in the case of the nailed joint. In the cases of the taped joints and the joints with both tape and dowels, the slip displacement was smaller than that for the nailed joints, although it did increase slightly as the fatigue life increased. The results of an energy analysis showed that it is possible to estimate the

slip displacement δ_{\max} at fatigue failure from the results of static testing. Although not considered in this study, the creep performance of the joints under sustained loads is an important issue. It should be investigated in the near future.

REFERENCES

- Chui YH, Ni C, Jiang L (1998) Finite-element model for nailed wood joints under reversed cyclic load. *J Struct Eng* 124:96-103.
- Fukuta S, Nomura M, Nishizawa M, Yamasaki M, Sasaki Y (2013) Composition of wooden joint by double-faced tape and wood dowel. *Wood Industry* 68:55-59. In Japanese.
- Gong M, Smith I (2005) Effect of stress levels on compressive low-cycle fatigue behavior of softwood. *Holzforschung* 59:662-668.
- Japan Agricultural Standards (2013) Japan agricultural standards for structural panel. http://www.maff.go.jp/j/jas/jas_kikaku/pdf/kikaku_52.pdf (1 February 2016) (In Japanese).
- Li L, Gong M, Smith I, Li D (2012) Exploratory study on fatigue behavior of laterally loaded, nailed timber joints, based on a dissipated energy criterion. *Holzforschung* 66:863-869.
- McNatt LR (1978) Linear regression of fatigue data. *Wood Sci* 11:39-41.
- Ogawa K, Sasaki Y, Yamasaki M, Fukuta S (2015) Theoretical estimation of mechanical properties of plywood-sheathed shear wall with combined use of adhesive tape and wood dowels. *Wood Fiber Sci* 47:421-430.
- Sasaki Y, Oya A, Yamasaki M (2014) Energetic investigation of the fatigue of wood. *Holzforschung* 68:843-848.
- Sugimoto T, Sasaki Y, Yamasaki M (2007) Fatigue of structural plywood under cyclic shear through thickness I: Fatigue process and failure criterion based on strain energy. *J Wood Sci* 53:296-302.
- Wakashima Y, Hirai T (1993) Hysteretic properties of nailed timber-plywood joint under cyclic loading I: Static cyclic loading test. *Mokuzai Gakkaishi* 39:1259-1266. In Japanese.
- Watanabe A, Sasaki Y, Yamasaki M (2014) Bending fatigue of wood: Strain energy-based failure criterion and fatigue life prediction. *Wood Fiber Sci* 46:216-227.